IEEE Sensors Journal, vol.-, no.-, pp.-, 2015, in press

Temperature Modulated Gas Sensing E-nose System for Low-cost and Fast Detection

Xin Yin, Lei Zhang, *Member, IEEE,* Fengchun Tian, and David Zhang, *Fellow, IEEE*

***Abstract*—Constant sensor-heating voltage is commonly used in electronic nose, such that multiple sensors should be integrated as a sensor array in order to differentiate multiple odor analytes. However, supplying a constant heating voltage for each sensor cannot provide rich pattern information, resulting in high cost and weak capability of an E-nose in detection. To address this issue, this work aims at introducing an optimal temperature modulation technique of gas sensors for achieving low-cost, fast and accurate detection. The contributions of this paper include: 1) the temperature modulated gas sensing system proposed in this work operates in a linearly dynamical region by generating a linear control signal waveform of sensors' heating voltage. 2) With a highly-efficient extreme learning machine that follows a random projection based learning mechanism, the proposed system is developed for simultaneous gas classification and gas concentration prediction. 3) The optimal heating voltage analysis of gas sensors is explored by using machine learning methods for providing some perspective and insight for optimal heating voltage selection. Experimental results and comparisons in terms of gas classification accuracy, concentration prediction error, system cost and power consumption significantly demonstrate the high precision and efficacy of our proposed E-nose system. The data is available in http://www.escience.cn/people/lei/index.html**

***Index Terms*—Electronic nose, temperature modulation, gas detection, extreme learning machine**

I. Introduction

ELECTRONIC nose (E-nose), as a typical machine olfaction application, is a gas sensing system consisting of a metal oxide semiconductor gas sensor array and a pattern recognition unit. E-nose technology has been widely applied in different fields during recent years. In environmental controls, Lamagna *et al*. [1] used an E-nose to characterize emissions from a highly polluted river. Yang *et al*. [2] used electronic nose based on porous In_2O_3 microtubes sensor array to discriminate VOCs. The recent work of E-nose for detection of gases includes [3, 4, 5, 37]. In medical diagnosis, Roine *et al*. [6] realize the detection of Prostate Cancer by electronic nose. Jia *et al*. [7] used an electronic nose to discriminate bacterial types of wound infections. Westenbrink *et al*. [8] developed a new electronic nose instrument to detect colorectal cancer. In agricultural area, Hui *et al*. [9] forecast the quality of winter jujube by electronic nose. Pan *et al*. [10] combined electronic nose and gas chromatography mass spectrometry to realize the early detection and classification of pathogenic fungal disease in post-harvest strawberry fruit. In food quality and security field, Yang, *et al*. [11] applied electronic nose to discriminate and characterize different intensities of goat flavor in goat milk. Wei et al. [12] used electronic nose to detect the internal quality of peanuts during storage. Brudzewskim *et al*. [30] applied a differentiated electronic nose to recognize the quality of coffee. In environmental monitoring, a portable E-nose instrument for gas classification was designed in [26], which contains QCM sensors. Leo *et al*. [36] proposed a large-scale sensor array data with an artificial olfactory system and explored the data processing method for mixture detection. Lujan *et al*. [40] proposed a calibration system of sensors using the minimal number of experiments and SVM. In our previous study [22], an IAQ (Indoor Air Quality) E-nose was built to monitor gases qualitatively and quantitatively with a MOS sensor array.

In our existing E-nose, a prototype of IAQ detection device was provided [25]. By using MOS sensor array and machine learning algorithms, classification and prediction of indoor air contaminants can be implemented in diffusion way. However, the cost and power consumption of an E-nose, especially for the sensor array, are still relatively high for real-time users. With the motivation of achieving low-cost and fast IAQ detection, this work applied a novel extreme learning machine and temperature self-modulation in order to narrow down the scale of sensor array, without degrading the prediction performance.

Temperature modulation is a known technique during recent years. The physicochemical mechanism on sensor film surface under temperature modulation was discussed in [13, 27], which show the temperature dependence of MOS sensors [28]. Also in [29], a model is proposed to predict the behavior of sensors exposed to CO and O_2 during fast temperature variations. Due to the improved selectivity of sensors, temperature modulation technique was used in various applications, such as fish spoilage evaluation [14], quantitative analysis of pesticide residue [31], and odor recognition [15, 16, 18, 21, 32, 33, 34]. Fonollosa *et al*. [35] proposed a temperature optimization of metal oxide sensors based on mutual information for improving the odor recognition performance. Generally, there are many

Manuscript received June 8, 2015. This work was supported by National Natural Science Foundation of China (61401048), the 2013 Innovative Team Construction Project of Chongqing Universities, Hong Kong Scholar Program (XJ2013044), China Postdoctoral Science Foundation (2014M550457), and Chongqing University Postgraduates' Innovation Fund (CDJXS12161106). *(Corresponding author: Lei Zhang.)*

X. Yin, L. Zhang and F. Tian are with College of Communication Engineering, Chongqing University, China (e-mail: yxsuixinliutang@sina.com; leizhang@cqu.edu.cn; fengchuntian@cqu.edu.cn)

D. Zhang is with Department of Computing, The Hong Kong Polytechnic University, Hong Kong (e-main:csdzhang@comp.polyu.edu.hk)

branches for the research of temperature modulation, such as heating voltage optimization, selection of waveform, modulation with feedback structure, and feature extraction, etc.

The motivation of this paper is to lower the system cost but with high precision of detection. Technically, we modulate sensors to narrow down the scale of sensor array for low-cost by introducing an easily transferred temperature modulation technique. We treat the sensor at different temperature as a virtual sensor, such that we can obtain more information by scanning the temperature range. A detailed analysis of the optimal heating voltage is given in Section IV.D. In this work, a new temperature modulated E-nose system of low cost, low energy consumption and high efficiency, is proposed in this paper for gas sensing application (e.g. IAQ monitoring).

In our proposed E-nose system, several widely used learning techniques are systematically investigated. Among machine learning theory, support vector machine/regression (SVM/SVR) and BP neural network (BP-NN) were widely used in many fields. However, BP-NN is prone to get trapped in local minima for complex regression problems, so that a local optimal solution is commonly obtained. Besides, due to the random generated initial connected weights in BP-NN, different solutions are to be solved in gradient descent based searching. Support vector machines perform structural risk minimization in the framework of regularization theory, which can obtain unique globally optimal solution with a convex optimization problem. Similar to SVM, extreme learning machine (ELM) was proposed for solving a single-layer feed-forward network (SLFN), which has been proven to be an very effective and efficient algorithm for pattern classification and regression in different fields [19, 20]. With least square loss defined in model, ELM can analytically determine the output weights between the hidden layer and the output layer by constructing a hidden matrix with a nonlinear and differentiable mapping function (e.g. sigmoid, radial basis function, etc.).

To prove the effectiveness of the proposed E-nose system, experiments on three gases were conducted. Several machine learning techniques mentioned above are implemented for simultaneous classification and concentration prediction using 5-fold cross-validation and *leave-one-out* cross-validation strategies, respectively. The merits of this paper include:

(1) A simple but effective and scalable temperature modulated gas sensing system is proposed for very low concentration detection and indoor air quality (IAQ) monitoring.

(2) The proposed E-nose system is a high precision and low-cost gas sensing system that only integrates two metal oxide semiconductor gas sensors for multi-gas detection.

(3) With a very highly-efficient extreme learning machine model (ELM), the proposed E-nose can well accomplish both qualitative classification and quantitative prediction tasks simultaneously in real-time.

(4) The proposed E-nose is of high precision in detection (e.g. classification & prediction) and of high competitiveness in speed, cost and power consumption.

The rest of this paper is organized as follows. In Section II, the proposed E-nose system and experiments are presented. In Section III, the methodology of some popular machine learning techniques are briefly reviewed. In Section IV, the results and comparisons are presented. Section V concludes the paper.

TABLE I
CHARACTERISTIC OF THE TWO SENSORS

Sensor type	Detection objectives
TGS2602	VOCs, odorous gases, gaseous air contaminants
TGS2620	Alcohol , organic solvent vapors

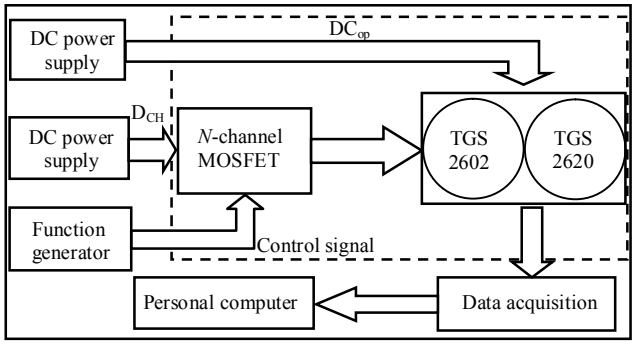

Fig. 1. Schematic diagram of temperature modulation gas sensing system

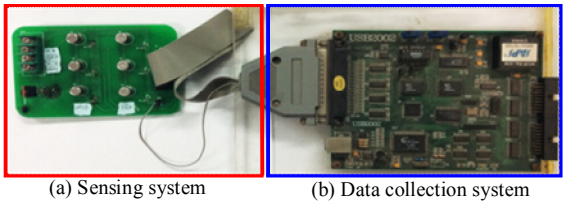

(a) Sensing system (b) Data collection system

Fig. 2. Temperature self-modulated gas sensing system. The left one is the sensor array system and the right one is the data collection system.

II. PROPOSED E-NOSE SYSTEM AND EXPERIMENTS

A. Proposed Temperature Self-modulated Gas Sensing System

Different from the existing E-nose system that the sensors work at constant heating voltage (e.g. 4V), a temperature modulation gas sensing system in an E-nose was proposed for IAQ monitoring, with block diagram shown in Fig.1. Generally, the system consists of three parts: voltage control (sensor temperature control), sensor array (TGS2620 and TGS2602) and data acquisition. In addition, a module (SHT2230 of Sensirion in Switzerland) with two auxiliary sensors for the temperature (T) and humidity (H) are used for compensation. Table I shows the function of the two sensors.

The printed circuit board (PCB) comprises of 2 semiconductor gas sensors (TGS2620, TGS2602), DC power supply interface, voltage control interface and data acquisition interface. The temperature self-modulated gas sensing system that comprises of integrated sensor circuits PCB board (left) and data acquisition (right) is shown in Fig.2. It is worth noting that 3 sensors of each type (three same sensor arrays) were integrated in practical PCB for avoiding the possible sensor fault. However, in algorithm analysis and monitoring, only one sensor array was used. In the voltage control part, two DC power modules (DF1730SB2A) are used to supply sensors' operating voltage and heating voltage through the DC power supply interface. For convenient description, DC_{op} (operating) and D_{CH} (heating) are nominated. DC_{op} is directly connected to the operating voltage pin of gas sensors, while D_{CH} is connected to the drain electrode of the *N*-channel MOSFET (IRF1010E),

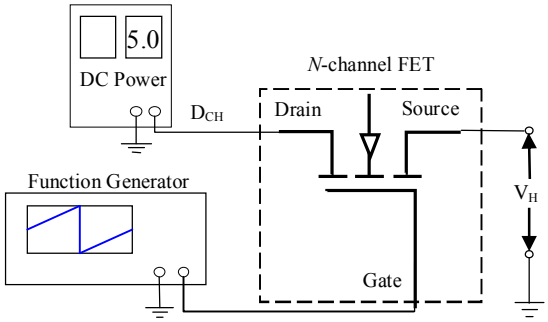

Fig. 3. Electrical circuit for generating modulated heating voltage

operating in a linear region, the source electrode is connected to the heating voltage pin of gas sensors, and the grid electrode is connected to an arbitrary function generator (AFG310) for generating control signal. Specifically, the electrical circuit for generating modulated heating voltage is shown in Fig.3. Thus, heating voltage can be controlled by changing the output signal of the function generator. Data acquisition is accomplished by an A/D sampling card (USB2002) (see the right part in Fig.2), which transfers data to PC through USB cable.

The reasons for selection of the TGS2620 and TGS2602 are:

- The two sensors show better stability with experience of our existing E-nose.
- TGS2201 in the existing E-nose has only one voltage pin, such that the heating and working voltage use the same pin, which is unstable if modulated. Besides, the recommended voltage of TGS2201 is 7v, while that of the others' are 5V. Therefore, a power chip can be omitted for lower cost.
- TGS2620 and TGS2602 have wider detection range and higher sensitivity for multiple gases monitoring due to their characteristic of broad spectrum response.

B. Experimental Setup and Data Acquisition

The experimental platform mainly consists of the proposed temperature self-modulated gas sensing system, temperature and humidity controlled gas sampling chamber (LRH-150-S) with a volume of 150L, humidifier, test gas bag, flow meter, air pump, standard target gas detector, standard temperature-humidity detector, etc. The specific experimental setup is shown in Fig.4. The humidifier is for adjusting the ambient condition of the gas chamber. The air pump is used to pumping test gas into chamber and the flow meter (100L/h) is used to control the gas injection velocity. The function of the mixing fan (3000rpm/min) is to keep the gas uniformly distributed in the chamber. The concentration of the injected gas in the chamber is obtained via the standard instrument, such as PPM, which is made by PPM Technology company. It is developed based on electrochemical sensor with voltage output and an approximately linear model embedded inside. The temperature and humidity in the chamber are measured by a temperature-humidity detector (APRESYS-TH).

Before the experiment, we first let the system operate at a stable heating voltage (usually 4v) for 1 hour, and then set the function generator as ramp function with suitable bias, amplitude and frequency, such that a ramp heating waveform can be obtained, where the voltage increases linearly from 3v up to 5v whose frequency is 20mHz. The sensing experiments in this paper can be summarized into three steps: *first*, set the

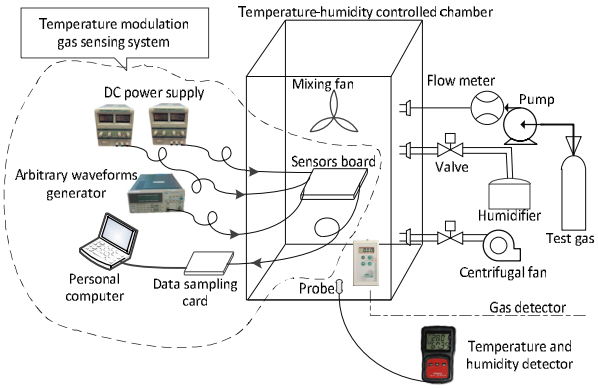

Fig. 4. E-nose experimental platform of the proposed system

target temperature and humidity of the gas sampling chamber; *second*, turn off the control power of the temperature and humidity in the chamber and begin to collect data continuously for 30 minutes, during which the target gas should be injected every 5 minutes. During data collection, gas concentration, ambient temperature and humidity should be recorded per minute; *third*, clean the chamber using clean air and return the first step to conduct the next experimental cycle.

For each experiment, 30 minutes (1800 seconds) will be taken for samples collection. The sensor response data can be divided in multiple periods according to the modulated heating period. In this study, three common indoor air contaminants such formaldehyde (HCHO), nitrogen dioxide (NO_2) and carbon monoxide (CO) were selected for IAQ monitoring application by using our proposed E-nose system. For each gas, samples were collected under different ambient conditions (i.e. temperature and humidity). Specifically, 10, 15, 20, 25, 30 and 35℃ are considered as target temperatures. 40%, 50%, 60% and 70% are considered as target humidity. The number of samples for HCHO, NO_2 and CO is 100, 113 and 96, respectively. The concentration of each sample with target temperature (T) and relative humidity (H) for three target gases is presented in Table II. We can see that the distribution of the concentration is almost uniformly configured from low to high concentration. The concentration range for HCHO samples and NO_2 samples are between 0 and 3 ppm, and the concentration range of CO samples is between 0 and 100 ppm. Additionally, the sensor response in one experimental cycle with 1800s is illustrated in Fig.5 (a), (b) and (c), which show the sensor response curve of multiple continuous periods (multiple samples) for each gas.

In addition, to show the sensor response curve under different gases, the sampling rate of sensor response is set to 100 Hz, such that 5000 sampling points will be obtained for each sample. The sensor response curves of TGS2620 and TGS2602 under three different gases are shown in Fig.6(a), which shows that under the temperature modulation of sensors' heating voltage, the patterns for different gases are visually separated. For statistical data analysis, principal component analysis (PCA) [39] is used. The PCA scatter diagram of all samples for three gases is shown in Fig.6(b), which shows that the gases can be separated, but HCHO and NO_2 are weakly overlapped. PCA is for dimension reduction but not for classification, therefore, classification techniques (e.g. SVM) should be used for pattern classification and regression.

TABLE II
THE TEMPERATURE, HUMIDITY AND CONCENTRATION INFORMATION OF THE EXPERIMENTAL DATA

Formaldehyde (HCHO) *samples*: concentrations under different target temperature and humidity (T,H) (concentration unit: ppm)														
(15,75)	(15,70)	(15,65)	(15,60)	(20,65)	(20,60)	(20,55)	(25,65)	(25,60)	(25,55)	(25,50)	(25,45)	(30,50)	(30,55)	(30,45)
0.97	0.90	0.75	0.63	1.29	0.58	0.44	1.77	1.36	0.72	0.05	1.25	1.27	0.73	0.88
0.91	1.11	0.78	0.54	1.55	1.16	1.68	1.22	1.08	0.56	1.44	2.01	1.09	0.18	0.72
1.16	0.51	1.00	0.43	1.16	1.04	1.77	1.20	1.10	1.27	0.99	0.51	1.91	1.88	0.47
1.37	1.41	0.86	0.67	0.87	0.75	1.59	0.89	1.34	0.74	0.79	0.83	0.85	1.39	1.14
1.73	2.06	0.84	0.98	0.57	0.49	2.30	2.44	1.98	0.76	1.49	2.29	0.09	1.84	0.40
-	-	0.53	1.42	1.03	-	1.60	2.01	0.88	0.52	0.71	1.95	1.55	0.91	0.60
-	-	-	-	-	-	-	0.97	1.50	1.82	1.31	0.73	1.06	0.63	-
-	-	-	-	-	-	-	-	1.32	1.16	0.62	1.23	1.38	0.79	-
Carbon monoxide (CO) samples (concentration unit: ppm)														
13.0	5.00	23.0	66.0	15.0	88.0	51.0	53.0	76.0	70.0	20.0	87.0	46.0	46.0	11.0
32.0	17.0	13.0	54.0	35.0	70.0	1.00	22.0	63.0	59.0	58.0	70.0	30.0	27.0	10.0
49.0	32.0	42.0	42.0	52.0	17.0	32.0	8.00	46.0	46.0	44.0	54.0	30.0	8.00	66.0
68.0	44.0	87.0	34.0	66.0	30.0	8.00	23.0	27.0	47.0	30.0	35.0	10.0	75.0	61.0
83.0	61.0	70.0	3.00	78.0	44.0	97.0	-	-	25.0	17.0	10.0	30.0	59.0	53.0
53.0	70.0	34.0	13.0	83.0	51.0	80.0	-	-	30.0	5.00	51.0	-	6.00	44.0
51.0	-	-	34.0	65.0	100.0	66.0	-	-	64.0	30.0	11.0	-	-	32.0
-	-	-	-	46.0	44.0	47.0	-	-	-	41.0	76.0	-	-	20.0
Nitrogen oxide (NO_2) samples (concentration unit: ppm)														
1.43	1.77	0.45	2.10	1.89	1.78	1.87	1.40	2.08	0.95	2.00	1.98	1.93	1.89	0.61
1.78	1.53	0.36	1.77	2.21	1.99	1.47	1.83	2.49	2.22	1.20	2.26	2.22	1.46	1.32
1.52	1.29	0.93	1.47	1.92	1.72	1.27	0.60	1.84	1.51	1.47	1.88	1.80	1.64	1.50
1.66	1.06	0.77	2.10	2.44	1.29	0.55	2.37	2.14	1.13	1.03	0.35	2.06	1.10	0.89
1.43	0.90	0.88	1.21	2.11	1.45	2.28	1.54	2.01	1.31	1.25	2.18	1.60	1.20	0.97
1.77	1.23	1.25	1.82	2.42	2.14	2.00	1.41	1.76	0.80	0.76	1.80	1.86	0.61	-
1.49	1.06	0.76	2.17	2.11	1.24	1.67	1.64	1.60	0.94	0.91	2.06	-	-	-
1.63	1.69	1.05	1.36	1.56	1.04	0.89	1.27	1.82	1.66	0.25	1.66	-	-	-

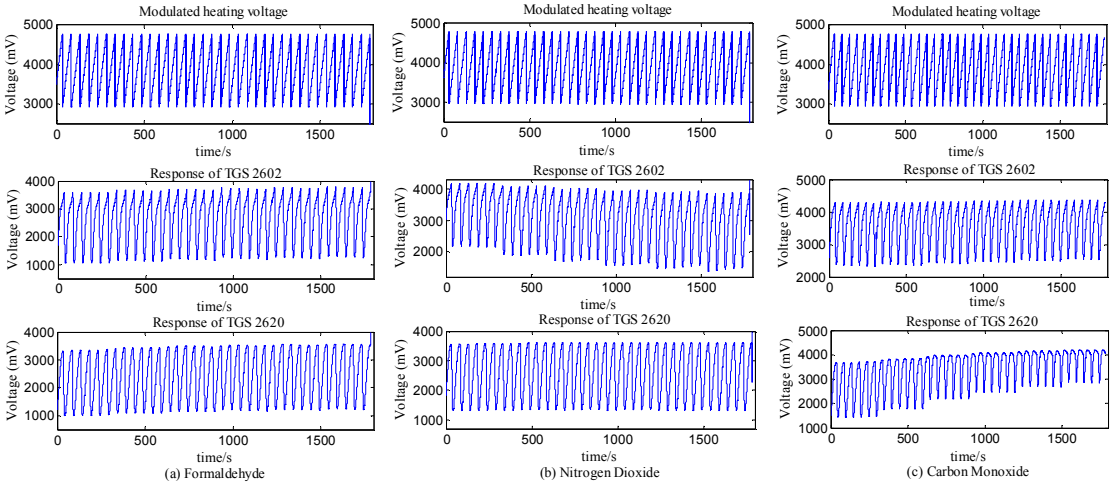

Fig. 5. Temperature-modulated sensor response curves for [0.03, 0.56, 1.08, 1.20, 1.6, 1.68] ppm formaldehyde (a), [0.05, 0.35, 0.91, 1.25, 1.47, 2.0] ppm Nitrogen dioxide (b) and [0.06, 8, 27, 46, 63, 76] ppm Carbon monoxide (c) gases in one experimental cycle (i.e. 6 samples/1800s)

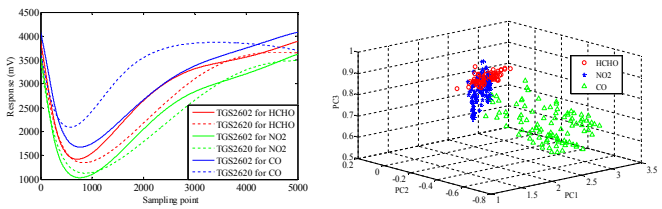

(a) Modulated sensor signal (b) PCA scatter points (PC1: 81.1%; PC2: 13.3%; PC3: 2.9%)

Fig. 6. Sensor response by modulating the heating voltage from 3v to 5v (a) and PCA result (b)

III. CLASSIFICATION AND REGRESSION METHODOLOGY

In this section, we briefly review back-propagation artificial neural network (BP-ANN), support vector machine/regression (SVM vs. SVR) and extreme learning machine (ELM).

A. BP-ANN

BP-ANN is one kind of neural network trained by gradient descent based back-propagation algorithm (BP). It has been widely used in pattern recognition and function approximation. However, BP-ANN is still with some inherent flaws. First, BP algorithm can easily get trapped in local minima for solving complex non-convex function approximation problems [23]. Second, the solutions are not stable due to the randomly generated initial weights and bias. Third, the training phase is time consuming due to its slow convergence in gradient search.

B. SVM and SVR

Support vector machines (SVM) perform structural risk minimization in the framework of regularization theory [24].

For linearly inseparable cases, SVM applies a non-linear kernel function to transform the input space to a higher dimensional feature space, such that the classes may be linearly separable and prior to calculate the separating hyper-plane. The kernel function can be sigmoid function, Gaussian radial basis function (RBF), etc. The brief principle of SVM is as follows.

Given a dataset $\mathbf{X} = [\mathbf{x}_1, \mathbf{x}_2, \cdots, \mathbf{x}_N]$ consisting of N samples and their corresponding label $[t_1, t_2, \cdots, t_N]$, where $\mathbf{x}_i = [x_{i1}, x_{i2}, \cdots, x_{in}]^{\mathrm{T}} \in \mathbf{R}^n, i = 1, \cdots, N$ and $t_i \in \{+1, -1\}$. The separating hyperplane can be defined as $\mathbf{W}^{\mathrm{T}}\mathbf{X} + \mathbf{b} = \vec{\mathbf{0}}$, where $\mathbf{W} \in \mathbf{R}^n$ is the normalized vector of hyper-plane and $\mathbf{b}$ is the bias. The goal of SVM is to maximize the distance $\frac{2}{\|\mathbf{W}\|^2}$ between hyperplane and the two classes, which is equivalent to minimize $\frac{1}{2}\|\mathbf{W}\|^2$. Therefore, the optimization problem of a linear SVM can be formulated as follows.

$$\min_{\mathbf{W}} \frac{1}{2}\|\mathbf{W}\|^2 \tag{1}$$
$$\text{s.t. } y_i[\mathbf{W}^{\mathrm{T}}\mathbf{x}_i + b] - 1 \geq 0, i = 1, \cdots, N$$

The dual optimization of (1) is generally solved in SVM.

The decision function of SVM for classification of an observation $\mathbf{x}$ can be formulated as

$$f(\mathbf{x}) = \mathrm{sign}\big((\mathbf{W}^{\mathrm{T}}\mathbf{x}) + b\big) = \mathrm{sign}\big(\textstyle\sum_{i=1}^{m} \boldsymbol{\alpha}^* y_i \big(\mathbf{x}_i^{\mathrm{T}}\mathbf{x}\big) + b^*\big) \tag{2}$$

where $\mathrm{sign}(\cdot)$ denotes symbol function. Note that (2) belongs to a linear SVM. For linearly inseparable case (i.e. nonlinear problem), a non-linear function $\varphi(\cdot)$ can be used to map data into a feature space of high dimensionality, however, it is not explicit. With Mercer condition, kernel function, represented by inner product $\langle \varphi(\mathbf{x}_i), \varphi(\mathbf{x}) \rangle$, is introduced. Then the decision function (6) can be written as

$$f(\mathbf{x}) = \mathrm{sign}(\textstyle\sum_{i=1}^{m} \boldsymbol{\alpha}^* y_i \varphi(\mathbf{x}_i)^{\mathrm{T}} \varphi(\mathbf{x}) + b) \tag{3}$$

Note that $\varphi(\mathbf{x}_i)^{\mathrm{T}}\varphi(\mathbf{x}_i)$ can be used as kernel function $\kappa(\mathbf{x}, \mathbf{x}_i)$.

Support vector regression (SVR) is used for solving function approximation problems, which is an extension of SVM.

C. ELM

Extreme learning machine (ELM) was proposed to solve a single-layer feed-forward network, which has been proven to be an effective and efficient algorithm for pattern classification and regression [19, 20, 38]. ELM can analytically determine the output weights (solutions) between the hidden layer and the output layer using Moore–Penrose generalized inverse by adopting the least square loss of prediction error, which then involves solving a regularized least square problem efficiently in closed form. The brief principle of ELM for multi-class classification is presented as follows.

Given a dataset $\mathbf{X} = [\mathbf{x}_1, \mathbf{x}_2, \cdots, \mathbf{x}_N]$ of N samples and the ground truth is denoted as $[\mathbf{t}_1, \mathbf{t}_2, \cdots, \mathbf{t}_N]$, where each data $\mathbf{x}_i = [x_{i1}, x_{i2}, \cdots, x_{in}]^{\mathrm{T}} \in \mathbf{R}^n$ and $\mathbf{t}_i = [1,0,\cdots,0]^{\mathrm{T}} \in \mathbf{R}^m, i = 1, \cdots, N$, if $\mathbf{t}_i$ belongs to the class 1. n and m denote the number of input and output neurons, respectively. Specifically, n is the number of dimension and m is the number of classes. The output matrix of the hidden layer with respect to $\mathbf{X}$ is denoted as $\mathbf{H} = H(\mathbf{W}\mathbf{X} + \mathbf{b}) \in \mathbf{R}^{N \times L}$, where L is the number of hidden nodes, $H(\cdot)$ is the activation function (e.g., RBF function, sigmoid function, etc.), $\mathbf{W} \in \mathbf{R}^{L \times n}$ is a randomly selected matrix, and $\mathbf{b} \in \mathbf{R}^L$ is the bias of hidden layer. The output weights between the hidden layer and the output layer being learned is denoted as $\boldsymbol{\beta} \in \mathbf{R}^{L \times m}$.

Algorithm 1. ELM algorithm

Input:
Training samples $\{\mathbf{X}_{\mathrm{tr}}, \mathbf{T}_{\mathrm{tr}}\}$, $\mathbf{X}_{\mathrm{tr}} \in \mathbf{R}^{n \times N}$, $\mathbf{T}_{\mathrm{tr}} \in \mathbf{R}^{N \times m}$.
The penalty constant C and the number of hidden nodes L.
Output:
The output weight matrix $\boldsymbol{\beta} \in \mathbf{R}^{L \times m}$.
Procedure:
1. Initialize the ELM network with random input weights $\mathbf{W} \in \mathbf{R}^{L \times n}$ and hidden bias $\mathbf{b} \in \mathbf{R}^L$.
2. Calculate the output matrix $\mathbf{H}$ of hidden layer as $\mathbf{H} = sigmoid(\mathbf{W}\mathbf{X}_{\mathrm{tr}} + \mathbf{B})$.
3. Compute the output weights $\boldsymbol{\beta}$ using (5).
end

Regularized ELM aims to solve $\boldsymbol{\beta}$ by minimizing the squared loss and the norm of $\boldsymbol{\beta}$, which is formulated as follows

$$\min_{\boldsymbol{\beta}} \; L_{\mathrm{ELM}} = \frac{1}{2}\|\boldsymbol{\beta}\|^2 + C \cdot \frac{1}{2}\textstyle\sum_{i=1}^{N}\|\xi_i\|^2 \tag{4}$$
$$s.t. \;\; \mathbf{H}(\mathbf{x}_i)\boldsymbol{\beta} = \mathbf{t}_i - \xi_i, i = 1, \cdots, N$$

where ξ_i denotes the prediction error with respect to the i th training pattern, and C is a penalty constant on the training errors. The solution $\boldsymbol{\beta}$ of (4) can be represented as

$$\boldsymbol{\beta}^* = \begin{cases} \left(\mathbf{H}^{\mathrm{T}}\mathbf{H} + \frac{\mathbf{I}_{L \times L}}{C}\right)^{-1} \mathbf{H}^{\mathrm{T}}\mathbf{T}, & \text{if } N \geq L \\ \mathbf{H}^{\mathrm{T}}\left(\mathbf{H}\mathbf{H}^{\mathrm{T}} + \frac{\mathbf{I}_{N \times N}}{C}\right)^{-1} \mathbf{T}, & \text{if } N < L \end{cases} \tag{5}$$

In decision of an observation $\mathbf{x}$, the predicted output of ELM can be obtained by feed-forward computation, i.e.

$$\mathbf{y}_{out} = H(\mathbf{W} \cdot \mathbf{x} + \mathbf{b})\boldsymbol{\beta}^* \tag{6}$$

More details of ELM theory can be referred as [19]. The ELM algorithm is summarized in Algorithm 1.

D. Model Establishment and Parameter Setting

MATLAB R2011b software is used to code and carry out all the algorithms for odor classification and concentration prediction. BP-ANN with one hidden layer is established by a built-in neural network toolbox using the "*trainlm*" algorithm. SVM/SVR is implemented by an open source LIBSVM toolbox. For BP-ANN, the number of hidden nodes is tuned from {5, 7, 8, 9}. For SVR/SVM, penalty factor C and kernel parameter G are optimized by using grid search method with cross-validation, where C and G are tuned from $\{2^{-8}, 2^{-7}, \ldots, 2^{8}\}$.

The ELM algorithm is implemented as Algorithm 1. Similarly, the parameters C (regularization coefficient) and L (the number of hidden nodes) are also optimized by grid search method, where C is tuned from $\{10^{-10}, 10^{-3}, \ldots, 10^{10}\}$, and L is tuned from $\{10, 10^2, 10^3, 10^4\}$.

All the algorithms mentioned above are evaluated in terms of the average classification accuracy (for qualitative odor classification) and prediction error (for quantitative concentration prediction) of 10 times cross-validation. Note that the prediction error is shown in three metrics, such as Mean absolute Relative Error (MRE), Mean Absolute Error (MAE) and Mean Square Error (MSE), which can be calculated by

$$\mathrm{MRE} = \frac{1}{n}\textstyle\sum_{i=1}^{n} |y_i - t_i|/t_i \times 100\% \tag{7}$$
$$\mathrm{MAE} = \frac{1}{n}\textstyle\sum_{i=1}^{n} |y_i - t_i| \tag{8}$$
$$\mathrm{MSE} = \frac{1}{n}\textstyle\sum_{i=1}^{n} (y_i - t_i)^2 \tag{9}$$

where y_i and t_i denote the predicted value and true value of the i-th sample, and n denote the number of test samples.

The pseudo-code of the cross-validation and grid search in evaluation is presented in Algorithm 2, which takes ELM as an example. For SVM/SVR, similar pseudo-code is used. For each

Algorithm 2. Grid search and cross-validation

Input: Data **X**, label vector **T**, parameter sets C, G, and L.
for i=$C_{\min}$:$C_{\max}$
  for j=$L_{\min}$:$L_{\max}$
    C=10^i;
    L=10^j;
    for repeat_time=1:10
      for cross_fold=1:N
        Training phase: *call* ELM **Algorithm 1**.
        Testing phase: Compute the output for each fold.
      end for
      Record the average results of cross-validation.
    end for
  end for
end for
Output: Classification accuracy, MRE, MAE, MSE.

method, the best results are reported in this paper. Note that for classification, 5-fold cross-validation is used; for concentration prediction *leaver-one-out* (LOO) cross-validation is used. The data partition of the 5-fold CV is illustrated in Fig.7.

E. On-line Usage for Real-time Application

First, the machine learning model (e.g. ELM) is trained off-line by solving Eq.(4). The well-trained model parameters **β** are then stored in E-nose system. Then, in real-time application, new sample **x** will be collected continuously by an E-nose, and the predicted label or concentration y is obtained via Eq.(6).

IV. Experimental Results

A. Feature Extraction

As shown in Fig.6(a), 5000 points are included in each modulated sensor response sequence in one sample, which demonstrates that the odor pattern is represented as a matrix (i.e. the row denotes the sensors and the column denotes the modulation). For convenient analysis, we uniformly *down-sample* K points with the same intervals in each sensor sequence (5000 points) of each sample, and concatenate the extracted points from the two sensors into a $2K$-dimensional feature vector of together with temperature and humidity for recognition of each sample. To explore the influence resulting from the number of sampling points in gas classification and concentration prediction, we have shown the results by changing the number K of sampling points for better insight of how the number of sampling points influences the performance in part *C*. In this paper, we have discussed the results by tuning K=5,…,20. If K=5, for example, the 1th, 1001th, 2001th, 3001th and 4001th points would be selected. Note that the sensor response, measured temperature and humidity have been normalized into [0,1] in data processing.

B. Qualitative Classification

In this work, three kinds of different contaminants are involved, which is recognized as a multi-class problem. The experiments by using BP-ANN, SVM and ELM algorithms are established. Under the framework of Algorithm 2, the average accuracies of 5-fold cross-validation for each method with the best parameters are provided in Table III. From this table, we can see that all methods can classify these three gases quite well. For CO, 100% accuracy can be obtained by three algorithms, and it is consistent with the PCA result in Fig.6(b) that the cluster of CO is separated from others.

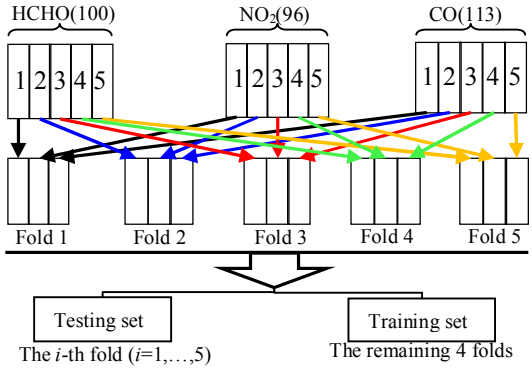

Fig. 7. Data partition scheme for 5-fold cross-validation

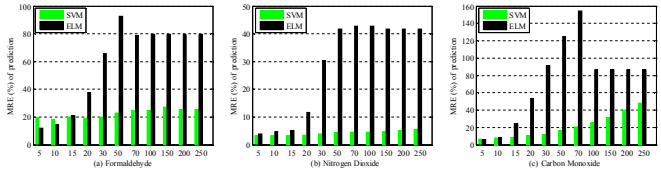

Fig. 8. MREs with different number of sampling points by using SVM and ELM methods. The digits in x-axis denote the number of sampling points.

We can also see that HCHO can be accurately identified with 100% by SVM and ELM, and BP-ANN becomes slightly weaker. For NO_2, the classification accuracies for all methods are more than 99%. We see that for both SVM and ELM, a larger penalty parameter C is more beneficial to the model. Additionally, ELM shows better recognition ability when the number of sampling points is equal to 5, 10, and 15. The results from different learning models demonstrate that the proposed temperature self-modulated gas sensing system is very effective for representing odor patterns.

C. Quantitative Concentration Prediction

For quantitative analysis, we present the concentration prediction of HCHO, NO_2 and CO by using BP-ANN, SVR and ELM, respectively. Fig.8 shows the error variation of MRE with the increasing number of sampling points by using SVM and ELM, due to their ability of fast implementation.

From Fig.8 we clearly observe that when the number of sampling points selected from the sensor response curve is larger than 20, higher MRE of prediction is obtained for each gas. This may be caused by redundant information (noises) when more sampling points are extracted as features, which are not beneficial to machine learning for prediction. Therefore, in this paper, we present the performance comparison of the proposed system in detail by determining K as 5, 10, 15, and 20, respectively. Numerically, the average MRE, MAE, MSE and their standard deviation (i.e. Std) of 10 times running by using *leave-one-out* cross-validation strategy for three gases are reported in Table IV, from which we can have the following observations:

- For HCHO, ELM obtains the lowest MRE (11.98%) of prediction, and the mean absolution error (MAE) is 0.1ppm, when the number K of sampling points is less than 10.
- For NO_2, SVR obtains the lowest prediction error of 3.18% and the MAE of prediction is 0.034ppm. The prediction error of ELM is slightly higher than SVR.
- For CO, ELM still performs the best result with MRE of

TABLE III
CLASSIFICATION ACCURACY OF ALL ALGORITHMS BY USING OUR PROPOSED E-NOSE SYSTEM

Number of Sampling Points	Model	Parameters	Average accuracy of 5-fold cross-validation			
			Formaldehyde (%)	Nitrogen oxide (%)	Carbon monoxide (%)	Average
5	BP-ANN	Hidden nodes=5	99.07	98.96	100.0	99.34
	SVM	C=7, G=0	100.0	97.60	100.0	99.20
	ELM	C=10, L=3	**100.0**	**99.92**	**100.0**	**99.97**
10	BP-ANN	Hidden nodes=7	99.43	100.00	100.0	99.81
	SVM	C=8, G=0	100.0	98.40	100.0	99.47
	ELM	C=7, L=3	**100.0**	**99.60**	**100.0**	**99.87**
15	BP-ANN	Hidden nodes=8	99.43	99.52	100.0	99.65
	SVM	C=8, G=0	100.0	98.40	100.0	99.47
	ELM	C=9, L=3	**100.0**	**99.60**	**100.0**	**99.87**
20	BP-ANN	Hidden nodes=9	99.14	99.84	100.0	99.66
	SVM	C=8, G=-2	**100.0**	**99.20**	**100.0**	**99.73**
	ELM	C=10, L=3	100.0	97.92	100.0	99.31

TABLE IV
CONCENTRATION PREDICTION PERFORMANCE FOR FORMALDEHYDE (HCHO), NITROGEN DIOXIDE (NO2) AND CARBON MONOXIDE (CO) CONTAMINANTS WITH LEAVE-ONE-OUT (LOO) CROSS-VALIDATION

Gas	Formaldehyde (HCHO)							
K	Model	Parameters	MRE (%)	Std	MAE (ppm)	Std	MSE (ppm^2)	Std
5	BP-ANN	Hidden nodes=5	17.55	3.07	0.11	0.005	0.020	0.0025
	SVR	C=8, g=3	19.68	0	0.11	0	0.022	0
	ELM	***C*=8, *L*=3**	**11.98**	**0.30**	**0.10**	**0.001**	**0.016**	**0.0005**
10	BP-ANN	Hidden nodes=7	17.55	2.28	0.11	0.007	0.020	0.0023
	SVR	C=8, g=3	18.15	0	0.10	0	0.017	0
	ELM	C=9, L=4	14.29	0.62	0.09	0.001	0.015	0.0007
15	BP-ANN	Hidden nodes=8	19.45	3.10	0.11	0.010	0.020	0.0030
	SVR	C=7, g=3	20.00	0	0.10	0	0.017	0
	ELM	C=9, L=4	20.69	0.86	0.15	0.002	0.034	0.0009
20	BP-ANN	Hidden nodes=9	18.06	2.67	0.11	0.008	0.019	0.0020
	SVR	C=8, g=2	18.50	0	0.10	0	0.017	0
	ELM	C=10, L=3	37.61	2.12	0.20	0.008	0.074	0.0070
Gas	Nitrogen Dioxide (NO_2)							
K	Model	Parameters	MRE (%)	Std	MAE (ppm)	Std	MSE (ppm^2)	Std
5	BP-ANN	Hidden nodes=5	7.14	0.5	0.080	0.004	0.010	0.0011
	SVR	C=9, g=4	3.29	0	0.036	0	0.002	0
	ELM	C=10, L=3	3.81	0.15	0.040	0.001	0.003	0.0002
10	BP-ANN	Hidden nodes=7	7.54	0.57	0.085	0.005	0.012	0.0010
	SVR	***C*=9, g=3**	**3.18**	**0**	**0.034**	**0**	**0.002**	**0**
	ELM	C=10, L=3	4.63	0.11	0.050	0.001	0.005	0.0003
15	BP-ANN	Hidden nodes=8	7.40	0.57	0.085	0.006	0.011	0.0015
	SVR	C=9, g=2	3.29	0	0.035	0	0.002	0
	ELM	C=9, L=4	5.25	0.16	0.056	0.001	0.006	0.0002
20	BP-ANN	Hidden nodes=9	7.54	0.49	0.085	0.005	0.012	0.0017
	SVR	C=9, g=2	3.46	0	0.036	0	0.002	0
	ELM	C=10, L=3	11.7	0.56	0.110	0.006	0.020	0.0020
Gas	Carbon Monoxide (CO)							
K	Model	Parameters	MRE (%)	Std	MAE (ppm)	Std	MSE (ppm^2)	Std
5	BP-ANN	Hidden nodes=5	5.83	1.26	0.10	0.006	0.016	0.0016
	SVR	C=8, g=2	6.25	0	1.43	0	4.120	0
	ELM	***C*=9, *L*=4**	**5.48**	**0.32**	**0.97**	**0.030**	**1.560**	**0.120**
10	BP-ANN	Hidden nodes=7	5.62	1.03	0.10	0.006	0.016	0.002
	SVR	C=7, g=2	7.64	0	1.85	0	6.770	0
	ELM	C=9, L=4	8.61	0.96	1.21	0.060	2.430	0.210
15	BP-ANN	Hidden nodes=8	5.73	0.49	0.10	0.005	0.016	0.002
	SVR	C=7, g=2	8.57	0	1.82	0	6.140	0
	ELM	C=8, L=4	24.3	1.92	4.17	0.160	28.87	2.080
20	BP-ANN	Hidden nodes=9	5.58	1.00	0.10	0.009	0.015	0.002
	SVR	C=6, g=2	10.3	0	2.46	0	11.99	0
	ELM	C=10, L=4	53.6	6.83	9.45	0.730	141.0	21.35

5.48%, and MAE of 0.97ppm. BP-ANN ranks the second.

- The MRE, MAE, MSE increase with the rising of sampling points for SVM and ELM, which demonstrates that a smaller number of sampling points can better represent odors.

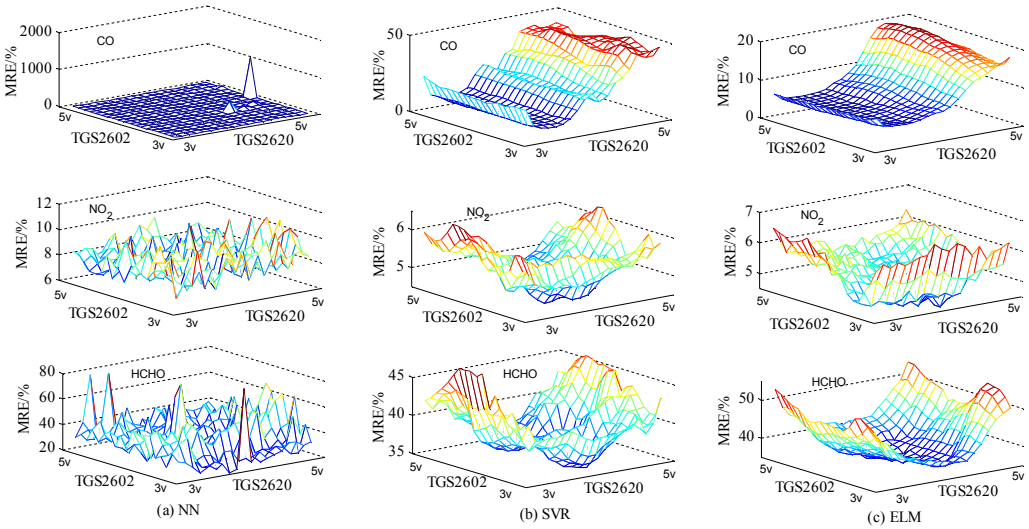

Fig. 9. Performance analysis with different heating voltage for each sensor based on three algorithms.

D. *Optimal Sensor Heating Voltage Analysis*

In this section, grid search method is used to analyze the prediction performance variation with different heating voltages of gas sensors. To observe the optimal heating voltage of each sensor, one sampling point between 3v and 5v with uniform interval is extracted from each sensor, then the three algorithms are implemented. The performance for each method is described in 3-D plots with TGS2620 (x-axis), TGS2602 (y-axis) and MRE (z-axis) shown as Fig.9(a), (b) and (c), respectively. We have the following observations:

- For BP-ANN method, the optimal heating voltages of sensors with lower MRE are not obvious. This demonstrates that NN is not sensitive to the change of sensors' heating voltage.
- For SVR and ELM, the optimal heating voltages of TGS2620 and TGS2602 have similar characteristic. It's clearly observed that the optimal voltage region for NO_2 and HCHO is in the middle part of the two sensors.
- From the 3-D curves of SVR and ELM, the near-optimal heating voltage of TGS2620 is 3.3v and 4v for CO and HCHO, respectively. For NO_2, the near-optimal heating voltage of TGS2602 is 3.3v.

It is worth noting that the correlation between the heating voltage and temperature of sensors has been studied in [17]. The relation between temperature and the sensor resistance was demonstrated to be approximately and inversely linear. The heating voltage is exponentially proportional to the heating temperature of sensors. The sensor array with modulation can produce richer patterns of gases than the same array without modulation, due to that temperature modulation can change the sensitive resistance of gas sensors.

Note that the temperature modulation is a dynamical process, while the traditional single working temperature is static which is shown in Fig.10. Therefore, the "4v" in temperature modulation is not seriously equivalent to the "4v-constant" in traditional way. However, the optimal sensor heating voltage analysis is to provide a deep insight of the paper motivation. Thus, the performance analysis in Fig.9 by scanning the voltage for each sensor is rational for observing the optimal heating voltage. The results can clearly show that the heating voltage of gas sensors has very important impact on the recognition performance of an E-nose. That is, temperature modulation is necessary and important for improving the performance of electronic noses. It is worth noting that the slight difference between temperature self-modulation (dynamical) and temperature modulation (static) lies in the modulation mechanism.

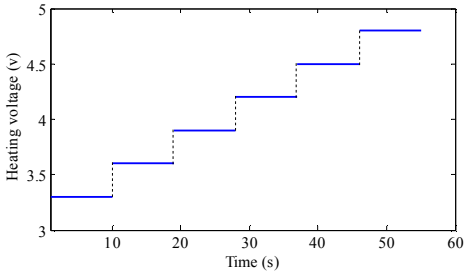

Fig. 10. Conventional temperature modulation process

E. *Performance Comparison*

The comparisons between the existing E-nose [22] and the proposed temperature self-modulated gas sensing system in this work are presented in Table V. For the proposed system, the results of ELM are presented for the proposed system. The classification accuracy of the existing E-nose based on SVM can be found in [3]. Besides, the relative prediction error of existing E-nose can be found in [25], in which the best result using PSOAGS-BP is compared in this paper. The results in Table V show that the proposed gas sensing system achieves better performance than the existing E-nose system in classification, prediction, cost and power consumption. In production, the existing E-nose can be improved by adding a MOSFET and controlling the heating voltage by signal via I/O port of MCU. Note that the $\Delta Cost$ and $\Delta Power\text{-}consumption$ denote the differences in cost and power consumption between the proposed system and the existing system. We can observe that the cost and power consumption of the proposed system is near 50% lower than the existing system.

TABLE V
PERFORMANCE COMPARISONS BETWEEN OUR EXISTING E-NOSE AND THE PROPOSED GAS SENSING SYSTEM

System	Classification accuracy (%)				Prediction error, MRE (%)				$\Delta Cost$	$\Delta Power\ consumption$
	Method	HCHO	NO2	CO	Method	HCHO	NO2	CO		
Previous [3, 25]	HSVM	94.23	83.33	100	PSOAGS-BP	17.56	5.49	7.80	46%	50.7%
The proposed	ELM	100	99.92	100	ELM	11.98	3.18	5.48		

V. CONCLUSION AND FUTURE WORK

In this work, a temperature self-modulated gas sensing system is proposed in E-nose system for IAQ monitoring application. Temperature modulation is realized by generating a periodic ramp signal to control the output of the *N*-channel MOSFET, operating in a linear region. In the proposed cost-driven IAQ E-nose system, two metal oxide semiconductor gas sensors are used to represent and differentiate the patterns of multiple gases.

The differences between this work and others are three-fold:

- Our E-nose system is designed to operate in indoor environment, therefore the gas concentrations in our corresponding experiments are relative low according to the IAQ detection standard (i.e. the concentration should be less than 0.075ppm, 0.049ppm and 8.0ppm for formaldehyde, nitrogen dioxide and carbon monoxide, respectively, for a standard IAQ). On the contrary, the concentrations in other literatures are really high. For examples, the concentration is about 10^5 ppm in [15], 25-100 ppm in [18], 10-250 ppm in [32], and 200-400 ppm in [33].
- The modulation method in the proposed gas sensing system is designed as simple as possible, such that the existing E-nose can be extended by adding a MOSFET, whose output can be linearly controlled by generating a signal from MCU.
- Extreme learning machine, as a novel brain-alike learning technique, is incorporated into our E-nose system for fast pattern classification and concentration prediction.

Experiments on three air contaminants including HCHO, NO_2 and CO are conducted for data acquisition and performance analysis. For algorithm analysis, several popular machine learning techniques such as BP-ANN, SVM/SVR and ELM are used in this work for recognition and concentration prediction. Results indicate that it is practical and beneficial to apply temperature self-modulation technique in E-nose system for IAQ monitoring. Additionally, the optimal heating voltages of sensors for different gases are also analyzed in Fig.10, which clearly demonstrates the optimal heating voltage regions of sensors. In the future, we will conduct more experiments on other contaminants and new machine learning models for further showing the effectiveness and efficiency of our proposed E-nose system.

ACKNOWLEDGMENT

The authors would like to express their sincere appreciation to the associate editor and anonymous experts for their valuable comments in their busy time.

REFERENCES

[1] A. Lamagna, S. Reich, D. Rodrigurez, A. Boselli, D. Cicerone, "The use of an electronic nose to characterize emissions from a highly polluted river," Sensors and Actuators B, vol. 131, pp. 121–124, 2008.

[2] W. Yang, P. Wan, M.Y. Jia, J. Hu, Y.F. Guan, L. Feng, "A novel electronic nose based on porous In2O3 microtubes sensor array for the discrimination of VOCs," Biosensors and Bioelectronics, vol. 64, pp. 547-553, Feb 2015.

[3] L. Zhang, F.C. Tian, H. Nie, L.J. Dang, G.R. Li, Q. Ye, C. Kadri, "Classification of multiple indoor air contaminants by an electronic nose and a hybrid support vector machine," Sensors and Actuators B: Chemical, vol. 174, pp. 114-125, Nov 2012.

[4] L. Zhang, F.C. Tian, S.Q. Liu, J.L. Guo, B. Hu, Q. Ye, L.J. Dang, X.W. Peng, C. Kadri, J.W. Feng, "Chaos based neural network optimization for concentration estimation of indoor air contaminants by an electronic nose," Sensors and Actuators A: Physical, vol. 189, pp. 161-167, Jan 2013.

[5] H. Liu, R. Chu, and Z. Tang, "Metal Oxide Gas Sensor Drift Compensation Using a Two-Dimensional Classifier Ensemble," Sensors, vol. 15, no. 5, pp. 10180-10193, 2015.

[6] A. Roine, E. Veskimäe, A. Tuokko, P. Kumpulainen, J. Koskimäki, T. A. Keinänen, M. R. Häkkinen, J. Vepsäläinen, T. Paavonen, J. Lekkala, T. Lehtimäki, T. L. Tammela, N. K.J. Oksala, "Detection of Prostate Cancer by an Electronic Nose: A Proof of Principle Study," The Journal of Urology, vol. 192, no. 1, pp. 230-235, Jul 2014.

[7] P.F. Jia, F.C. Tian, Q.H. He, S. Fan, J.L. Liu, Simon X. Yang, "Feature extraction of wound infection data for electronic nose based on a novel weighted KPCA," Sensors and Actuators B: Chemical, vol. 201, pp. 555-566, Oct 2014.

[8] E. Westenbrink, R.P. Arasaradnam, N. O'Connell, C. Bailey, C. Nwokolo, K.D. Bardhan, J.A. Covington, "Development and application of a new electronic nose instrument for the detection of colorectal cancer," Biosensors and Bioelectronics, Oct 2014.

[9] G.H. Hui, J.J. Jin, S.G. Deng, X.Ye, M.T. Zhao, M.M. Wang, D.D. Ye, et al. "Quality forecasting method based on electronic nose," Food Chemistry, vol. 170, pp. 484-491, Mar 2015.

[10] L.Q. Pan, W. Zhang, N. Zhu, S.B. Mao, K. Tu, "Early detection and classification of pathogenic fungal disease in post-harvest strawberry fruit by electronic nose and gas chromatography–mass spectrometry," Food Research International, vol. 62, pp. 162-168, Aug 2014.

[11] C.J. Yang, W. Ding, L.J. Ma, R. Jia, "Discrimination and characterization of different intensities of goaty flavor in goat milk by means of an electronic nose," Journal of Dairy Science, vol. 98, no. 1, pp. 55-67, Jan 2015.

[12] Z.B. Wei, J. Wang, W.L. Zhang, "Detecting internal quality of peanuts during storage using electronic nose responses combined with physicochemical methods," Food Chemistry, vol. 177, pp. 89-96, Jun 2015.

[13] A.P. Lee, B.J. Reedy, "Temperature modulation in semiconductor gas sensing," Sensors and Actuators B: Chemical, vol. 60, no. 1, pp. 35-42, Nov 1999.

[14] A. Perera, A. Pardo, D. Barrettino, A. Hierlermann, S. Marco, "Evaluation of fish spoilage by means of a single metal oxide sensor under temperature modulation," Sensors and Actuators B: Chemical, vol. 146, no. 2, pp. 477-482, Apr 2010.

[15] R. Gosangi, R. Gutierrez-Osuna, "Active temperature modulation of metal-oxide sensors for quantitative analysis of gas mixtures," Sensors and Actuators B: Chemical, vol. 185, pp. 201-210, Aug 2013.

[16] F. Hossein-Babaei, A. Amini, "Recognition of complex odors with a single generic tin oxide gas sensor," Sensors and Actuators B: Chemical, vol. 194, pp. 156-163, Apr 2014.

[17] E. Martinelli, D. Polese, A. Catini, A. D'Amico, C. Natale, "Self-adapted temperature modulation in metal-oxide semiconductor gas sensors," Sensors and Actuators B: Chemical, vol. 161, no. 1, pp. 534-541, Jan 2012.

[18] K. A. Ngo, P. Lauque, K. Aguir, "High performance of a gas identification system using sensor array and temperature modulation," Sensors and Actuators B: Chemical, vol. 124, no. 1, pp. 209-216, Jun 2007.

[19] G.B. Huang, Q.Y. Zhu, and C.K. Siew, "Extreme learning machine: Theory and applications," Neurocomputing, vol. 70, no. 1–3, pp. 489–501, Dec. 2006.
[20] G. Feng, G.-B. Huang, Q. Lin, and R. Gay, "Error minimized extreme learning machine with growth of hidden nodes and incremental learning," IEEE Trans. Neural Netw., vol. 20, no. 8, pp. 1352–1357, Aug. 2009.
[21] F. Herrero-Carrón, D.J. Yanez, F.D.B. Rodriguez, and P. Varona, "An active, inverse temperature modulation strategy for single sensor odorant classification," Sensors and Actuators B: Chemical, vol. 206, pp. 555-563, 2015.
[22] L. Zhang, F.C. Tian, "Performance Study of Multilayer Perceptrons in a Low-Cost Electronic Nose," IEEE Trans. Instrumentation and Measurement, vol. 63, no. 7, pp. 1670-1679, Jul 2014.
[23] S. Haykin, "Neural Networks: A Comprehensive Foundation," Prentice-Hall, New Jersey, 1999.
[24] C. Cortes and V. Vapnik, "Support vector networks," Mach. Learn., vol. 20, no. 3, pp. 273-297, 1995.
[25] L. Zhang, F. Tian, C. Kadri, G. Pei, H. Li, and L. Pan, "Gases concentration estimation using heuristics and bio-inspired optimization models for experimental chemical electronic nose," Sensors and Actuators B: Chemical, vol. 160, no. 1, pp. 760-770, 2011.
[26] A. Ozmen, and E. Dogan, "Design of a Portable E-Nose Instrument for Gas Classifications," IEEE Trans. Instrumentation and Measurement, vol. 58, no. 10, pp. 3609-361, 2009.
[27] P.K. Clifford, and D.T. Tuma, "Characteristics of semiconductor gas sensors II. transient response to temperature change," Sensors and Actuators, pp. 255-281, 1982.
[28] N. Bârsan, and A. Tomescu, "The temperature dependence of the response of SnO2-based gas sensing layers to O2, CH4 and CO," Sensors and Actuators B: Chemical, vol. 26, no. 1–3, pp. 45-48, 1995.
[29] A. Fort, S. Rocchi, M.B. Serrano-Santos, M. Mugnaini, V. Vignoli, A. Atrei, and R. Spinicci, "CO sensing with SnO2-based thick film sensors: Surface state model for conductance responses during thermal-modulation," Sensors and Actuators B: Chemical, vol. 116, no. 1–2, pp. 43-48, 2006.
[30] K. Brudzewski, S. Osowski, and A. Dwulit, "Recognition of Coffee Using Differential Electronic Nose," IEEE Trans. Instrumentation and Measurement, vol. 61, no. 6, pp. 1803-1810, 2012.
[31] X. Huang, L. Wang, Y. Sun, F. Meng, and J. Liu, "Quantitative analysis of pesticide residue based on the dynamic response of a single SnO2 gas sensor," Sensors and Actuators B: Chemical, vol. 99, no. 2–3, pp. 330-335, 2004.
[32] J.R. Huang, G.Y. Li, Z.Y. Huang, X.J. Huang, and J.H. Liu, "Temperature modulation and artificial neural network evaluation for improving the CO selectivity of SnO 2 gas sensor," Sensors and Actuators B: Chemical, vol. 114, no. 2, pp. 1059-1063, 2006.
[33] H. Ge, and J. Liu, "Identification of gas mixtures by a distributed support vector machine network and wavelet decomposition from temperature modulated semiconductor gas sensor," Sensors and Actuators B: Chemical, vol. 117, no. 2, pp. 408-414, 2006.
[34] F. Hossein-Babaei, A. Amini, "A breakthrough in gas diagnosis with a temperature-modulated generic metal oxide gas sensor," Sensors and Actuators B: Chemical, vol. 166-167, pp. 419-425, 2012.
[35] J. Fonollosa, L. Fernández, R. Huerta, A.G. Gálvez, S. Marco, "Temperature optimization of metal oxide sensor arrays using Mutual Information," Sensors and Actuators B: Chemical, vol. 187, pp. 331-339, 2013.
[36] M. Leo, C. Distante, M. Bernabei, K. Persaud, "An Efficient Approach for Preprocessing Data from a Large-Scale Chemical Sensor Array," Sensors, vol. 14, no. 9, pp. 17786-17806, 2014.
[37] S.K. Jha, K. Hayashi, "A Novel Odor Filtering and Sensing System Combined with Regression Analysis for Chemical Vapor Quantification," Sensors and Actuators B: Chemical, vol. 200, pp. 269-287, 2014.
[38] G.B. Huang, "An Insight into Extreme Learning Machines: Random Neurons, Random Features and Kernels," Cognitive Computation, vol. 6, pp. 376-390, 2014.
[39] I. Jolliffe, Principal Component Analysis, Wiley Online Library 2002.
[40] I.R. Lujan, J. Fonollosa, A. Vergara, M. Homer, R. Huerta, "On the calibration of sensor arrays for pattern recognition using the minimal number of experiments," Chemometrics and Intelligent Laboratory Systems, vol. 130, pp. 123-134, 2014.

Xin Yin received his BSc and MSc degree in Circuits and Systems from College of Communication Engineering, Chongqing University, Chongqing, China, in 2012 and 2015. He is now working in China Electronics Technology Group Corporation No.29 Research Institute. His research interests include hardware design, electronic nose technology and pattern recognition.

Lei Zhang received his Ph.D degree in Circuits and Systems from the College of Communication Engineering, Chongqing University, Chongqing, China, in 2013. From 2015, he is a Distinguished Research Fellow with Chongqing University. He was selected as a Hong Kong Scholar in China in 2013, and he is currently also a Post-Doctoral Fellow with The Hong Kong Polytechnic University, Hong Kong. He has authored more than 40 scientific papers in electronic nose, machine olfaction, pattern recognition, and machine learning. His current research interests include electronic noses, machine learning, pattern recognition and multi-sensor system. Dr. Zhang was a recipient of Outstanding Doctoral Dissertation Award of Chongqing, China, in 2015, Hong Kong Scholar Award in 2014, Academy Award for Youth Innovation of Chongqing University in 2013 and the New Academic Researcher Award for Doctoral Candidates from the Ministry of Education, China, in 2012.

Fengchun Tian received the Ph.D. degree in electrical engineering from Chongqing University, Chongqing, China, in 1997. He is currently a Full Professor with the College of Communication Engineering, Chongqing University. He has authored more than 100 publications in electronic nose, signal processing, and image processing. His current research interests include electronic nose technology, artificial olfactory systems, pattern recognition, chemical sensors, signal/image processing, wavelet, and computational intelligence. In 2006 and 2007, Professor Tian also worked as a part-time Professor with the University of Guelph, Canada.

David Zhang graduated in Computer Science from Peking University. He received his MSc in 1982 and his PhD in 1985 in Computer Science from the Harbin Institute of Technology (HIT), respectively. From 1986 to 1988 he was a Postdoctoral Fellow at Tsinghua University and then an Associate Professor at the Academia Sinica, Beijing. In 1994 he received his second PhD in Electrical and Computer Engineering from the University of Waterloo, Ontario, Canada. He is a Chair Professor since 2005 at the Hong Kong Polytechnic University where he is the Founding Director of the Biometrics Research Centre (UGC/CRC) supported by the Hong Kong SAR Government in 1998. He also serves as Visiting Chair Professor in Tsinghua University, and Adjunct Professor in Peking University, Shanghai Jiao Tong University, HIT, and the University of Waterloo. He is the Founder and Editor-in-Chief, International Journal of Image and Graphics (IJIG); Book Editor, Springer International Series on Biometrics (KISB); Organizer, the International Conference on Biometrics Authentication (ICBA); Associate Editor of more than ten international journals including IEEE Transactions and so on; and the author of more than **10** books, over **300** international journal papers and **30** patents from USA/Japan/HK/China. Professor Zhang is a Croucher Senior Research Fellow, Distinguished Speaker of the IEEE Computer Society, and a Fellow of both IEEE and IAPR.